Phytopathology • 2018 • 108:542-551 • https://doi.org/10.1094/PHYTO-09-17-0332-R

Bacteriology

e-Xtra*

Insights Into the Roles of Two Genes of the Histidine Biosynthesis Operon in Pathogenicity of *Xanthomonas oryzae* pv. *oryzicola*

Panpan Su, Zhiwei Song, Guichun Wu, Yancun Zhao, Yuqiang Zhang, Bo Wang, Guoliang Qian, Zheng Qing Fu, and Fengquan Liu†

First, second, fourth, and ninth authors: Institute of Plant Protection, Jiangsu Academy of Agricultural Science, Nanjing 210014, China; third, fifth, sixth, seventh, and ninth authors: College of Plant Protection, Nanjing Agricultural University, Nanjing 210095, China/Key Laboratory of Integrated Management of Crop Diseases and Pests (Nanjing Agricultural University), Ministry of Education, China; and eighth author: Department of Biological Sciences, University of South Carolina, Columbia.

Accepted for publication 15 December 2017.

ABSTRACT

Xanthomonas oryzae pv. *oryzicola* is an *X. oryzae* pathovar that causes bacterial leaf streak in rice. In this study, we performed functional characterization of a nine-gene *his* operon in *X. oryzae* pv. *oryzicola*. Sequence analysis indicates that this operon is highly conserved in *Xanthomonas* spp. Auxotrophic assays confirmed that the *his* operon was involved in histidine biosynthesis. We found that two genes within this operon, *trpR* and *hisB*, were required for virulence and bacterial growth in planta. Further research revealed that *trpR* and *hisB* play different roles in *X. oryzae* pv. *oryzicola*. The *trpR* acts as a transcriptional repressor and could negatively regulate the expression of *hisG*, *-D*, *-C*, *-B*, *-H*, *-A*, and *-F*. *hisB*, which encodes a bifunctional enzyme implicated in histidine biosynthesis, was shown to be required for xanthomonadin production in *X. oryzae* pv. *oryzicola*. The disruption of *hisB* reduced the transcriptional expression of five known shikimate pathway-related genes *xanB2*, *aroE*, *aroA*, *aroC*, and *aroK*. We found that the *his* operon in *X. oryzae* pv. *oryzicola* is not involved in hypersensitive response in nonhost tobacco plants. Collectively, our results revealed that two genes in histidine biosynthesis operon play an important role in the pathogenicity of *X. oryzae* pv. *oryzicola* Rs105.

Xanthomonas oryzae pv. *oryzicola* is a Gram-negative bacterium and the causal agent of bacterial leaf streak (BLS) of rice. *X. oryzae* pv. *oryzicola* causes significant economic losses in many rice growing countries in Asia annually, especially in China (Niño-Liu et al. 2006; Zhao et al. 2011). During infection, *X. oryzae* pv. *oryzicola* enters host plants mainly through stomata or wounds of the leaves and multiplies in the substomatal cavity. The colonization of *X. oryzae* pv. *oryzicola* in the intercellular spaces of the mesophyll, causes water-soaked interveinal lesions on rice leaves (Wang et al. 2007). This pathogen is characterized by typical yellow pigments known as xanthomonadins.

L-Histidine is one of the 20 natural amino acids found in proteins of living organisms. The side- chain of this amino acid consists of an imidazole ring and produces a pKa of 6.0; as such, histidine residues can act as an acid or a base in enzymatic reactions (Kulis-Horn et al. 2014; Polgár 2005; Rebek 1990).

L-histidine biosynthesis is a comprehensively elucidated ancient metabolic pathway present in different organisms. For decades, L-histidine biosynthesis has been investigated mainly in *Escherichia coli* and its close relative *Salmonella typhimurium*. Fundamental biological mechanisms, including operon structure, have been discovered. Moreover, histidine biosynthesis seems to be conserved in most organisms including bacteria, archaea, lower eukaryotes, and plants (Chapman and Nester, 1969; Fink 1964; Kulis-Horn et al. 2014; Lee et al. 2008; Stepansky and Leustek, 2006). Histidine biosynthesis pathway requires a series of 10 enzymatic reactions which transform the substrate ATP and phosphoribosyl pyrophosphate (PRPP) to become L-histidine (Alifano et al. 1996; Fani et al. 1995). In *E. coli* and *S. typhimurium*, the 10 enzymatic activities are encoded by eight genes, namely *hisA*, *-B*, *-C*, *-D*, *-F*, *-G*, *-H*, and *-IE*, which are organized in a single operon (Alifano et al. 1996; Carlomagno et al. 1988; Chiariotti et al. 1986; Fani et al. 1997; Fink 1964; Jung et al. 1998). Although *hisI* and *hisE* were considered two separate genes, further studies have confirmed that *hisI* and *hisE* are a single gene (Chiariotti et al. 1986).

Histidine biosynthesis plays an important role in cellular metabolism. Histidine biosynthesis and purine biosynthetic pathways are linked by 1-(5′-phosphoribosyl)-5-amino-4-imidazolecarboxamide (AICAR), a by-product of histidine synthesis and intermediate of purine biosynthesis (Bochner and Ames 1982; Klem and Davisson 1993; Papaleo et al. 2009). On the other hand, histidine biosynthesis is regulated not only by histidine, but also by other molecules. For example, the activity of the first enzyme of histidine biosynthesis is inhibited by histidine but is stimulated by PRPP and ATP (Alifano et al. 1996; Wiater et al. 1971). Under moderate amino acid starvation and in cells growing in a minimal medium, *his* operon expression is positively regulated by the alarmone guanosine 5′-diphosphate 3′-diphosphate (ppGpp), which is the effector of stringent responses (Alifano et al. 1996; Jung et al. 2010; Kulis-Horn et al. 2014).

Histidine biosynthesis in *X. oryzae* pv. *oryzicola* and other *Xanthomonas* spp. has been rarely explored. In *X. oryzae* pv. *oryzicola*, the histidine biosynthetic pathway also requires 10 enzymatic reactions, which are encoded by eight genes (*hisA*, *-B*, *-C*, *-D*, *-F*, *-G*, *-H*, and *-IE*), through BLAST search and KEGG pathway analysis (http://www.kegg.jp/kegg-bin/show_pathway?148397042654630/xor00340.args). Meanwhile, bioinformatics analysis shows that gene *trpR* (*XOC_2214*), which is upstream of *hisG*, encodes a transcriptional regulator. In this research, we identified two histidine biosynthesis related genes *trpR* and *hisB*, as important virulence determinants in *X. oryzae* pv. *oryzicola*. Our

†Corresponding Author: F. Liu; E-mail: fqliu20011@sina.com

First and second authors contributed equally to this work.

This work was supported by the National Natural Science Foundation of China (31371906; 31571974), Postdoctoral Foundation of Jiangsu Province (1601077C), and Special Fund for Agro-Scientific Research in the Public Interest (201303015).

*The *e-Xtra* logo stands for "electronic extra" and indicates that two supplementary figures and three supplementary tables are published online.

data revealed that *trpR* could negatively regulate the expression of *hisA*, *-B*, *-C*, *-D*, *-F*, *-G*, and *-H*. Furthermore, we also found that *hisB* affected the production of xanthomonadins in *X. oryzae* pv. *oryzicola*. To the best of our knowledge, this is the first study to perform a functional analysis of *trpR* and *hisB* in *Xanthomonas*.

MATERIALS AND METHODS

Bacterial strains, plasmids, and culture conditions. The information regarding the bacterial strains and plasmids related to this work is presented in Supplementary Table S1. All the *E. coli*

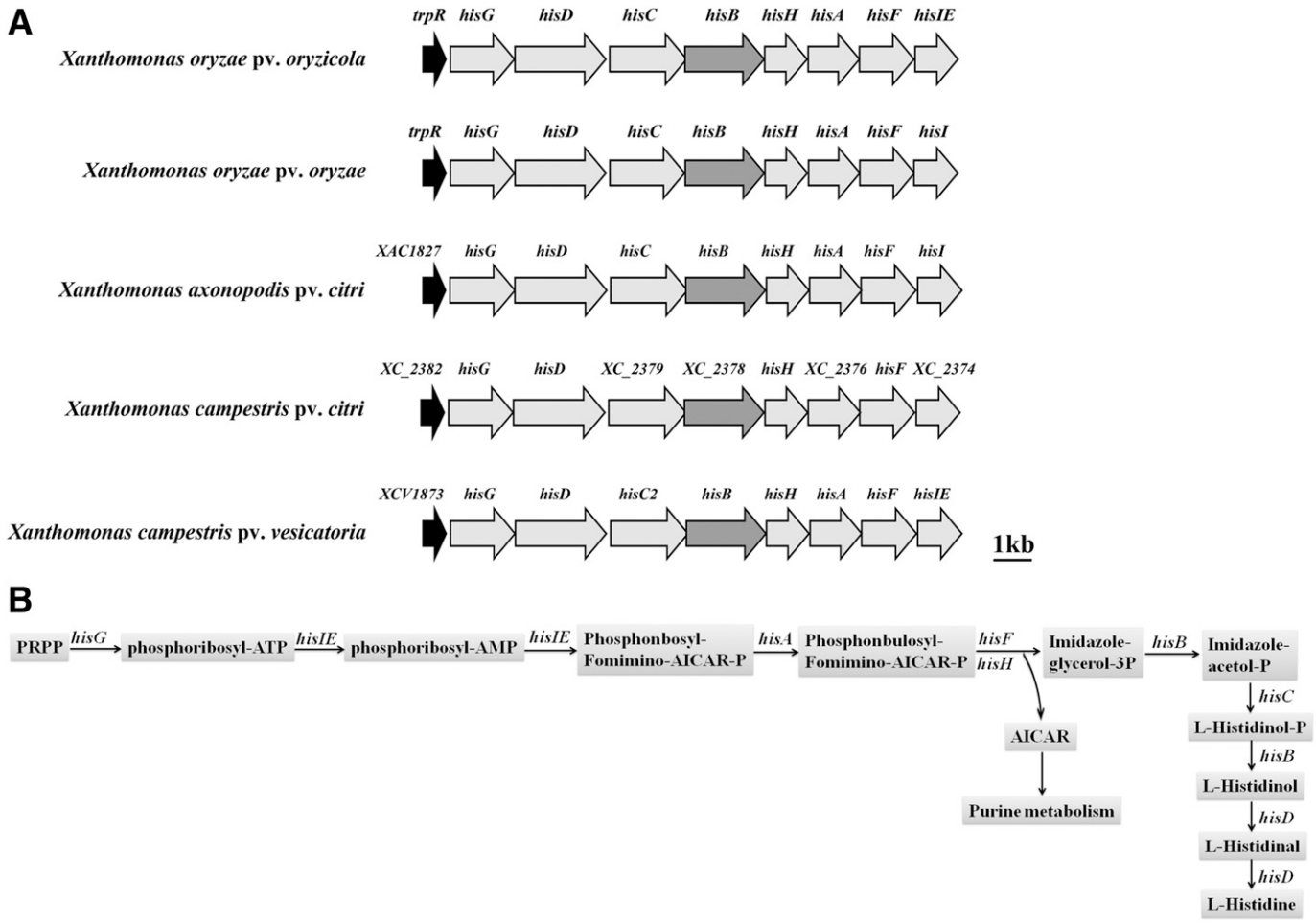

Fig. 1. Genetic structure of the *his* operon and metabolic pathway of histidine biosynthesis in *X. oryzae* pv. *oryzicola* and other related *Xanthomonas*. **A,** The direction of the arrow and the length of the box represent transcription direction and gene size. The data in this figure are based on GenBank database of *X. oryzae* pv. *oryzicola* BLS256, *X. oryzae* pv. *oryzae* PXO99^{A}, *X. axonopodis* pv. *citri* 306, *X. campestris* pv. *campestris* 8004, and *X. campestris* pv. *vesicatoria* 85-10. *XAC1827*, *XC_2382*, and *XCV1873* were the homologs of *trpR*. **B,** The metabolic pathway of histidine biosynthesis of *X. oryzae* pv. *oryzicola* (http://www.kegg.jp/). PRPP, phosphoribosyl pyrophosphate; AICAR, 1-(5-phosphoribosyl)-5-amino-4-imidazolecarboxamide.

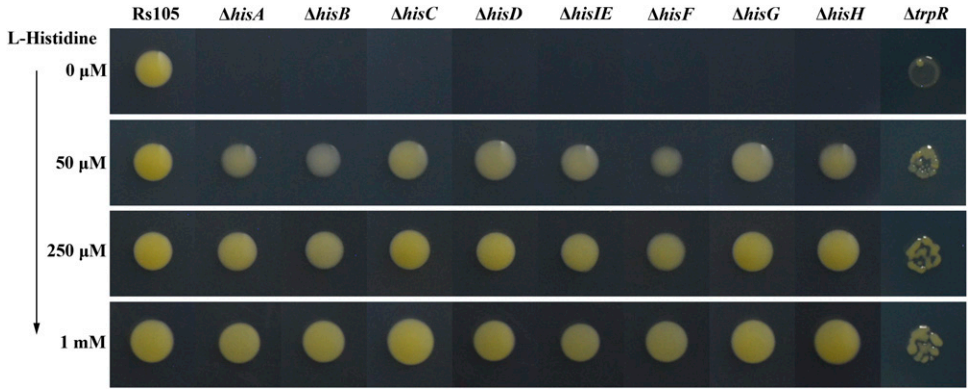

Fig. 2. Growth of *Xanthomonas oryzae* pv. *oryzicola* strains in XOM3 minimal medium supplemented with different concentrations of L-histidine. Bacterial cultures were spotted and cultured for 5 days at 28°C on XOM3 agar plates, which were supplemented with L-histidine with respective concentrations of 0 μM, 50 μM, 250 μM, and 1 mM. Rs105, the wild-type strain of *X. oryzae* pv. *oryzicola*; Δ*hisA*, the *hisA* deletion mutant; Δ*hisB*, the *hisB* deletion mutant; Δ*hisC*, the *hisC* deletion mutant; Δ*hisD*, the *hisD* deletion mutant; Δ*hisIE*, the *hisIE* deletion mutant; Δ*hisF*, the *hisF* deletion mutant; Δ*hisG*, the *hisG* deletion mutant; Δ*hisH*, the *hisH* deletion mutant; and Δ*trpR*, the *trpR* deletion mutant. Three replicates for each treatment were used, and the experiment was repeated three times. Data were from a representative experiment, and similar results were reported from two other independent experiments.

strains were cultivated at 37°C in Luria-Bertani (LB) broth or LB agar plates. Wild-type strain Rs105 of *X. oryzae* pv. *oryzicola* and its derivative strains were grown at 28°C in nutrient broth (NB) medium (beef extract, 3 g/liter; yeast extract, 1 g/liter; polypeptone, 5 g/liter; and sucrose, 10 g/liter) or on nutrient agar (NA) unless specified. XOM3 (1.8 g/liter D-xylose, 670 µM D, L-methionine, 10 µM sodium L-glutamate, 240 µM $NaFe^{2+}$-EDTA, 5 µM $MgCl_2$, 14.7 mM KH_2PO_4, 40 µM $MnSO_4$, pH 6.0) was used as minimal medium. Antibiotics were added to the medium as required, with the following final concentrations: ampicillin (Amp), 100 µg/ml; kanamycin (Kan), 50 µg/ml; and rifampicin (Rif), 100 µg/ml.

Generation of gene deletion mutants and complemented strains. The in-frame deletion mutants of target genes were generated from the *X. oryzae* pv. *oryzicola* wild-type Rs105 by allelic homologous recombination, and the suicide vector pK18mob*sacB* was used in the process (Qian et al. 2013a; Zhao et al. 2011; Zou et al. 2011). Two flanking regions of each gene were generated through PCR amplification by using different primer pairs. PCR fragments of each gene were digested with appropriate restriction enzymes and ligated into the vector pK18mob*sacB*, creating individual recombinant vectors. These recombinant vectors were transformed into wild-type Rs105 by electroporation, and NA plates lacking sucrose and supplemented Rif (100 µg/ml) and Km (50 µg/ml) were used to select transformants. Positive colonies were plated on NA plates containing 10% (wt/vol) sucrose and Rif (100 µg/ml) to select the second crossover events and these in-frame deletion mutants were confirmed through PCR (Supplementary Table S2). For complementation, each intact gene and the predicted promoter were amplified through PCR method using their corresponding primers, and were cloned into the complemented vector pUFR034 (De Feyter et al. 1990). The resultant constructs were transferred into the corresponding mutants by electroporation to generate these complemented strains and were confirmed through PCR, as previously described (Qian et al. 2013a; Zhao et al. 2011).

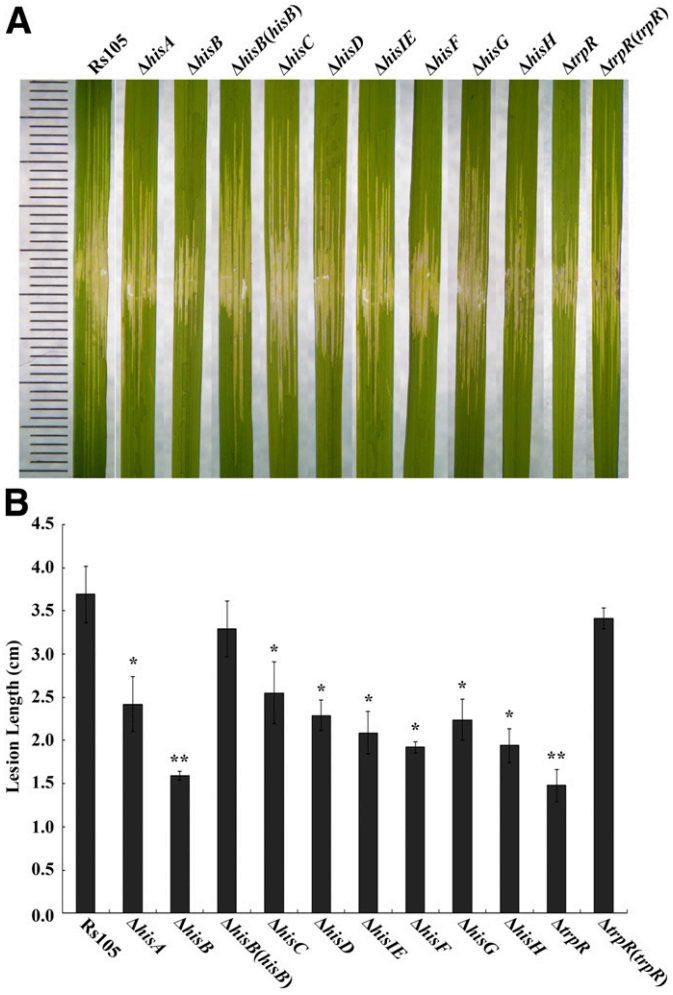

Fig. 3. Pathogenicity test of *Xanthomonas oryzae* pv. *oryzicola* strains in rice. **A,** Lesion lengths on the leaves of rice seedlings (cultivar Shanyou63, 2 weeks old) by infiltration with *X. oryzae* pv. *oryzicola* strains. **B,** Calculated data of lesion length on the leaves of rice seedlings (Shanyou63, 2 weeks old) inoculated with *X. oryzae* pv. *oryzicola* strains. Rs105, the wild-type strain of *X. oryzae* pv. *oryzicola*; Δ*hisA*, the *hisA* deletion mutant; Δ*hisB*, the *hisB* deletion mutant; Δ*hisB* (*hisB*), the complemented strain of Δ*hisB*; Δ*hisC*, the *hisC* deletion mutant; Δ*hisD*, the *hisD* deletion mutant; Δ*hisIE*, the *hisIE* deletion mutant; Δ*hisF*, the *hisF* deletion mutant; Δ*hisG*, the *hisG* deletion mutant; Δ*hisH*, the *hisH* deletion mutant; Δ*trpR*, the *trpR* deletion mutant; and Δ*trpR* (*trpR*), the complemented strain of Δ*trpR*. The experiment was repeated three times. Data were the means ± standard deviations from three repeats, each with 10 leaves. Vertical bars represent standard errors. * indicates differences between mutant and wild-type strain Rs105 at $P = 0.05$; ** indicates a significant difference between mutant and the wild-type Rs105 at $P = 0.01$.

Auxotrophic assays. The auxotrophic assays of each strain were performed as described previously with some modification (Park et al. 2007). In brief, *X. oryzae* pv. *oryzicola* strains were cultured in NB medium until midlogarithmic phase (optical density at 600 nm [OD_{600nm}] = 1.0). Cells were collected by centrifugation at 6,000 rpm and were washed twice with sterile ddH_2O. Each culture was resuspended with an equal volume of sterile ddH_2O. Then, 3 µl of bacterial cultures was spotted on XOM3 agar plates supplemented with L-histidine (Sigma) with respective concentrations of 0 µM, 50 µM, 250 µM, and 1 mM. The preparations were cultured for 5 days at 28°C. Experiments were repeated at least three times.

Pathogenicity assay and measurement of bacterial growth in planta. Pathogenicity assays were performed in a greenhouse at 22 to 30°C with a 70% relative humidity (Qian et al. 2013b; Zhao et al. 2011). In brief, wild-type (Rs105) and mutant strains were cultivated in NB medium at 28°C and 200 rpm. All strains were adjusted to a density of OD_{600nm} = 0.5 with ddH_2O. Bacterial suspension was infiltrated by using a needleless syringe and was inoculated into the 2-week-old rice leaves of cultivar Shanyou63 (susceptible to the pathogen). Each bacterium was inoculated into 10 leaves. The lesions length was measured after 10 days postinoculation, and representative leaves were collected for photos. The experiment was performed three times.

Measurement of bacterial growth in rice leaf tissue was carried out as described previously (Qian et al. 2013a; Zhao et al. 2012). Briefly, the study of the colonization of each *X. oryzae* pv. *oryzicola* strain was performed by homogenizing five inoculated leaves in 9 ml of sterile water. The leaves were cut in 6 mm sections around the inoculation spots after 1, 5, and 10 days after inoculation. After dilution of the homogenates, the resulting solutions were plated on NA plates supplemented with Rif (for the wild type and mutants). Each diluted homogenate was plated on three plates, respectively. The number of bacterial colonies on these plates was calculated after 2 days of incubation at 28°C. The experiment was performed three times.

HR assay. The HR (hypersensitive response, a programmed cell death) assay was performed as described previously (Zou et al. 2006). Briefly, the wild-type (Rs105) and mutant strains were cultured in NB medium at 28°C and 200 rpm. All the tested strains were cultured to a concentration of OD_{600nm} = 1.0 and centrifuged at 6,000 rpm to remove the culture medium. Cells were washed twice with sterile ddH_2O and were suspended in sterile ddH_2O with OD_{600nm} adjusted to 0.5. The bacterial suspension was infiltrated into the leaves of nonhost plant tobacco (*Nicotiana tabacum* L. 'Samsun') using needleless syringes. HR was observed and documented after 24 to 48 h of infiltration. The experiment was repeated three times.

Growth determination of Δ*trpR* and Δ*hisB* in XOM3 medium supplemented with different concentrations of

L-histidine. To confirm that *trpR* and *hisB* in *X. oryzae* pv. *oryzicola* were involved in histidine metabolism, we tested the growth rate of Δ*trpR* and Δ*hisB* in XOM3 medium, which were supplemented with different concentrations of L-histidine. In brief, *X. oryzae* pv. *oryzicola* strains were grown in NB broth at 28°C with shaking at 200 rpm. Cells were pelleted at the early logarithmic phase (OD_{600nm} = 0.5) by centrifugation at 6,000 rpm. Cells were washed twice with sterile ddH2O and were suspended in an equal volume of sterile ddH_2O. Then, a 300 µl of suspension was added into 30 ml of XOM3 medium supplemented with L-histidine (Sigma) at concentrations of 0 µM, 50 µM, 250 µM, and 1 mM. All inoculated broths were grown at 28°C with shaking at 200 rpm, and the OD_{600nm} value was determined every 8 or 12 h until bacterial growth reached the stationary stage.

Extraction and quantitative determination of the xanthomonadins. The extraction and determination of the xanthomonadins were performed as described previously in *X. campestris* pv. *campestris* (He et al. 2011). Briefly, *X. oryzae* pv. *oryzicola* wild-type strain and its derivative strains were grown in NB broth at 28°C with shaking at 200 rpm overnight. Two hundred-microliter aliquots of cells were transferred to 20 ml of freshly XOM3 broth supplemented with L-histidine and then cultured until the stationary phase OD_{600nm} reached 2.0. Cells were collected by centrifugation at 10,000 × *g* for 30 min and were resuspended in 1 ml of methanol. The suspension was shaken for 5 min at room temperature. Finally, a 100-µl aliquot of each extract was analyzed at an optical density of 445 nm (OD_{445nm}). The OD_{445nm} values obtained were used to determine the amount of xanthomonadins produced by each strain. The assay was performed three times, and the averages and standard deviations were calculated for each experiment.

Real-time PCR. Real-time PCR was performed according to a recent report in *X. oryzae* pv. *oryzae* (Liang et al. 2018), with minor modification. In brief, the experimental strains were grown in NB at 28°C with shaking at 200 rpm and cultured to OD_{600nm} = 1.0, and centrifuged at 6,000 rpm to remove culture medium. Cells were washed twice with ddH_2O, and then cell pellets were suspended in an equal volume of XOM3 broth. Cells of each strain were collected from XOM3 broth after treatment with L-histidine concentrations of 0 µM, 250 µM, and 1 mM for 3 h. RNA was isolated from *X. oryzae* pv. *oryzicola* under the guidance of instructions of the E.Z.N.A. Bacterial RNA Kit (OMEGA). According to the instructions of PrimeScript RT Reagent Kit (TaKaRa), RNA samples were initially treated with RNase inhibitors and DNaseI to remove gDNA. RNA integrity was then confirmed through electrophoresis by using 1.2% agarose gels, then 2 µg of each RNA sample was used to synthesize cDNA. The cDNA was subjected to quantitative real-time reverse transcription PCR (qRT-PCR) by using SYBR Premix EX Tag (TaKaRa) in an ABI PRISM 7500 Real-Time PCR System (Applied Biosystems), and 16S rRNA was used as an endogenous control. The primer sequences used in this assay are listed in Supplementary Table S3. The experiment was performed three times.

RESULTS

Analysis of the *his* operon in *Xanthomonas*. Using a BLASTP search, we analyzed the *his* operon in *X. oryzae* pv. *oryzicola* and other related species. As shown in Figure 1A, the *his* operon consists of eight genes (*hisA*, *-B*, *-C*, *-D*, *-F*, *-G*, *-H*, and *-IE*) in the available genome of *X. oryzae* pv. *oryzicola* BLS256. Meanwhile, in *X. oryzae* pv. *oryzicola*, *trpR*, a gene upstream of *hisG*, encodes a transcriptional regulator. The *trpR* gene was considered as part of the *his* operon. Sequencing analysis showed that the nine genes of *his* operon share the same transcriptional direction and are highly conserved in *X. oryzae* pv. *oryzae*, *X. axonopodis* pv. *citri*, *X. campestris* pv. *campestris*, and *X. campestris* pv. *vesicatoria.* The amino acid identity of each of the nine genes is above 80% between these *Xanthomonas* strains. These results suggest that the *his* operon may encode conserved functions in *Xanthomonas* spp. Meanwhile, it showed that the metabolic pathway of direct histidine biosynthesis from PRPP to L-histidine needed the participation of the enzymes encoded by the genes of *hisA*, *-B*, *-C*, *-D*, *-F*, *-G*, *-H*, and *-IE* in *X. oryzae* pv. *oryzicola* (Fig. 1B).

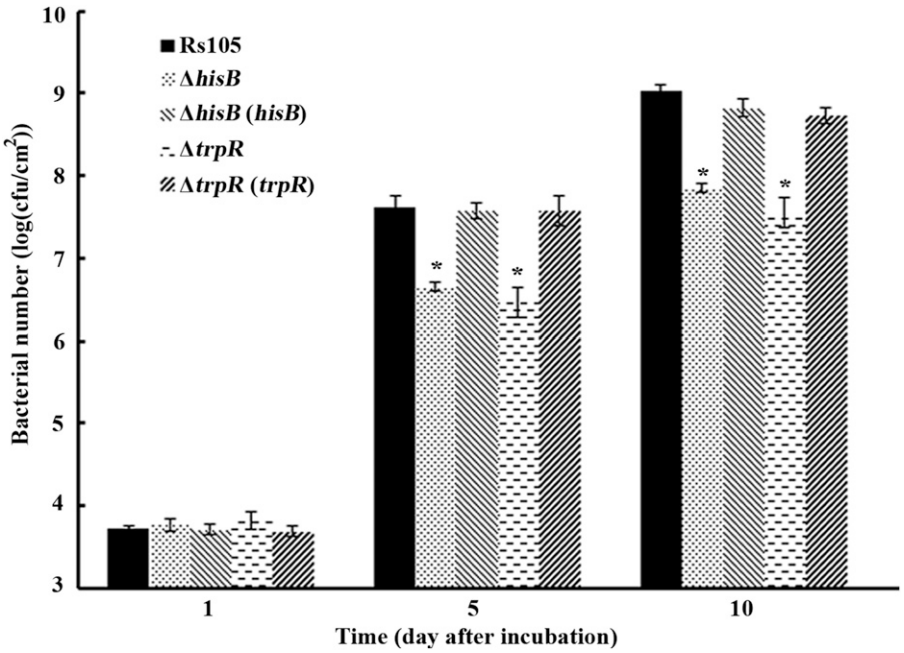

Fig. 4. *trpR* and *hisB* are required for the growth of *Xanthomonas oryzae* pv. *oryzicola* in planta. Bacterial cells were recovered from the infected rice leaves 1, 5, and 10 days after inoculation, and homogenized with sterile water. After dilution of the homogenates, the resulting solutions were plated on NA plates supplemented with Rif (for the wild type and mutants). The number of bacterial colonies on these plates was calculated after 2 days of incubation at 28°C. Rs105, the wild-type strain of *X. oryzae* pv. *oryzicola*; Δ*hisB*, the *hisB* deletion mutant; Δ*hisB* (*hisB*), the complemented strain of Δ*hisB*; Δ*trpR*, the *trpR* deletion mutant; Δ*trpR* (*trpR*), the complemented strain of Δ*trpR*. Three replicates for each treatment were used, and the experiment was repeated three times. Vertical bars represent standard errors. * indicates differences between mutant and wild-type strain Rs105 at P = 0.05.

***his* operon is essential for histidine biosynthesis in *X. oryzae* pv. *oryzicola*.** To confirm that the *his* operon in *X. oryzae* pv. *oryzicola* was involved in histidine biosynthesis, we tested the growth state of the mutants in XOM3 with different concentrations of L-histidine. The mutants, Δ*trpR*, Δ*hisA*, Δ*hisB*, Δ*hisC*, Δ*hisD*, Δ*hisIE*, Δ*hisF*, Δ*hisG*, and Δ*hisH*, were obtained as a result of the deletion of one gene of the *his* operon. Compared with the wild type which grew well in XOM3 medium without L-histidine, significant

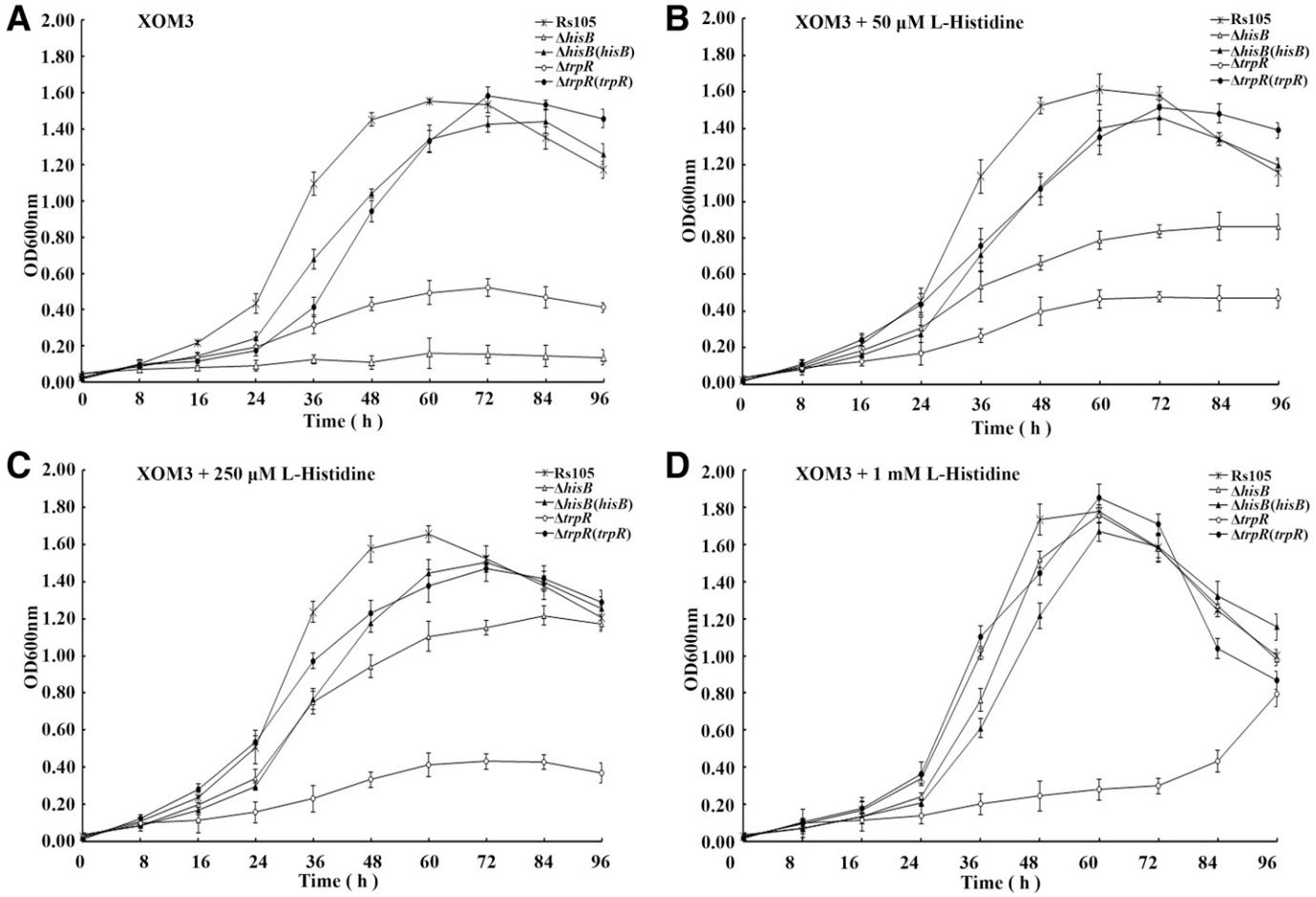

Fig. 5. Growth rate of the wild-type, mutant, and complemented strains in XOM3 minimal medium supplemented with different concentrations of L-histidine: **A,** XOM3; **B,** XOM3 + 50 μM L-histidine; **C,** XOM3 + 250 μM L-histidine; and **D,** XOM3 + 1 mM L-histidine. Rs105, the wild-type strain of *Xanthomonas oryzae* pv. *oryzicola*; Δ*hisB*, the *hisB* deletion mutant; Δ*hisB* (*hisB*), the complemented strain of Δ*hisB*; Δ*trpR*, the *trpR* deletion mutant; and Δ*trpR* (*trpR*), the complemented strain of Δ*trpR*. The optical density at 600 nm (OD_{600nm}) value was determined every 8 or 12 h until bacterial growth reached the stationary stage. Three replicates for each treatment were used, and the experiment was repeated three times. Vertical bars represent standard errors.

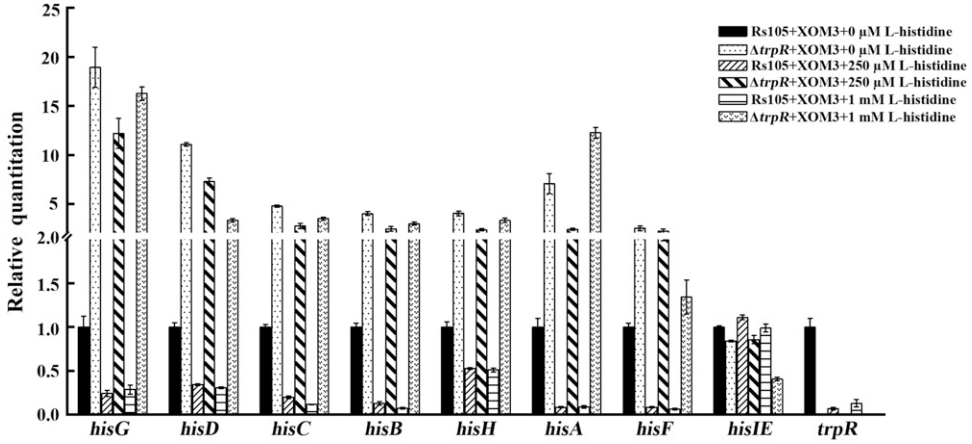

Fig. 6. *trpR* negatively regulates the expression of *hisG*, *-D*, *-C*, *-B*, *-H*, *-A*, *-F*, and the transcriptions of *hisG*, *-D*, *-C*, *-B*, *-H*, *-A*, *-F*, and *trpR* are inhibited by histidine. RNA was isolated from the cells of each strain, which were collected from XOM3 broth treated with 0 μM, 250 μM, and 1 mM L-histidine for 3 h. Quantitative real-time PCR was performed to analyze the expression levels of genes. Rs105, the wild-type strain of *Xanthomonas oryzae* pv. *oryzicola*; Δ*trpR*, the *trpR* deletion mutant. Data were the means ± standard deviations of triplicate measurements from a representative experiment, and similar results were reported from two other independent experiments. Vertical bars represent standard errors.

growth inhibition was observed in the *his* operon mutants (Fig. 2): single mutants of the eight *his* operon genes (Δ*hisA*, Δ*hisB*, Δ*hisC*, Δ*hisD*, Δ*hisIE*, Δ*hisF*, Δ*hisG*, and Δ*hisH*) showed no growth in XOM3 medium without supplementation of L-histidine after 5 days incubation at 28°C and one mutant, Δ*trpR*, showed significantly reduced growth. The inhibited growth in the *his* operon mutants could be restored by supplementing the XOM3 medium with 50 μM L-histidine. Δ*hisB* mutant appears as a white dot in the plate surface, whereas the wild-type bacteria and other mutant strains showed intense yellow color. This phenomenon showed that the *hisB* mutant lacked yellow pigmentation. In XOM3 media supplemented with 250 μM and 1 mM L-histidine, the growth states of all the mutants were similar in comparison with the wild-type strain. It must be noted that wild-type and mutant bacteria grew as single dots except for mutant Δ*trpR* (Fig. 2). The bacterial growth was restored in the corresponding complemented strains of the mutants of *trpR* and *hisB* (Supplementary Fig. S1). These results indicated that the *his* operon was involved in histidine biosynthesis in *X. oryzae* pv. *oryzicola*.

***trpR* and *hisB* are required for the full virulence and growth of *X. oryzae* pv. *oryzicola* in planta and the *his* operon is not necessary for triggering the HR in nonhost (plant) tobacco.** To determine whether *his* operon genes played a role in the virulence of *X. oryzae* pv. *oryzicola*, we compared the virulence of the mutants with wild type by injecting bacterial cells into the rice leaves using the inoculation concentration of OD_{600nm} = 0.5 (Qian et al. 2013a; Zhao et al. 2012). As shown in Figure 3A and B, all mutants exhibited decreased virulence in comparison with the wild-type Rs105, as reflected by the reduced length of water-soaking lesion symptoms. Meanwhile, the mutants of *trpR* and *hisB* exhibited a significant reduction in virulence, whereas their corresponding complemented strains retained almost full wild-type ability in this function. These results indicated that the *his* operon was required for bacterial endophytic life style. Since *hisB* mutant showed a stronger phenotype than other *his* genes mutants, and the *hisB* gene could have another implication in pathogenicity. Phenotype associated with *trp* mutant could also be associated with other virulence aspect.

In order to explore whether the roles of *trpR* and *hisB* in virulence were related with the proliferation of *X. oryzae* pv. *oryzicola* on host rice, we measured the growth ability of the mutants of *trpR* and *hisB* in the infected rice leaves. The bacterial cells were recovered from the infected rice leaves 1, 5, and 10 days after inoculation. As shown in Figure 4, Δ*trpR* and Δ*hisB* exhibited a significant decrease in cell numbers compared with the wild-type strain when were recovered

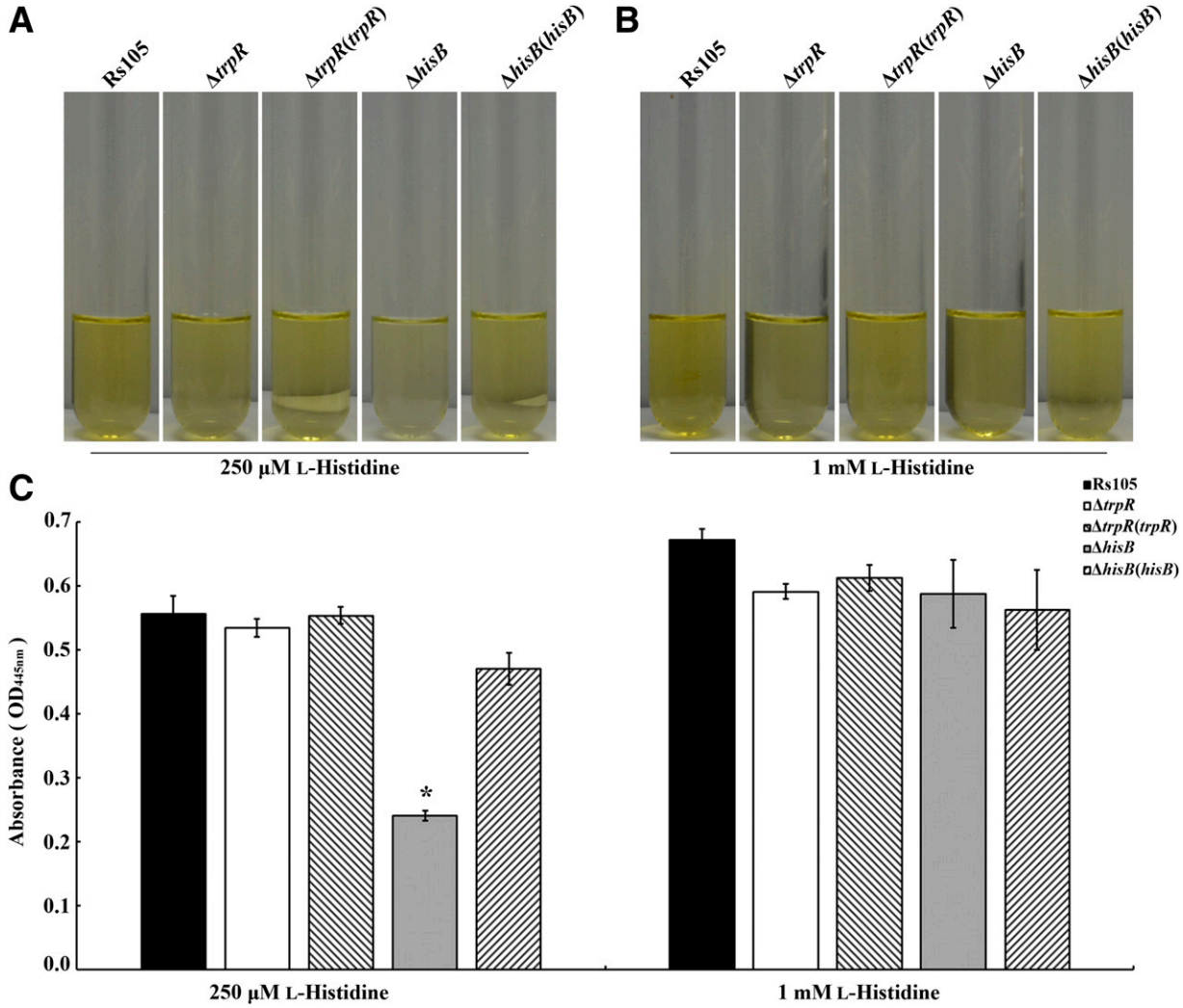

Fig. 7. Xanthomonadins production assay of the wild-type, mutant, and complemented strains. **A,** Representative results of extraction of xanthomonadins in *Xanthomonas oryzae* pv. *oryzicola* strains cultured in XOM3 broth supplemented with 250 μM L-histidine. **B,** Representative results of extraction of xanthomonadins pigment in *X. oryzae* pv. *oryzicola* strains cultured in XOM3 broth supplemented with 1 mM L-histidine. **C,** Calculated data of xanthomonadins production in *X. oryzae* pv. *oryzicola* strains. Rs105, the wild-type strain of *X. oryzae* pv. *oryzicola*; Δ*hisB*, the *hisB* deletion mutant; Δ*hisB* (*hisB*), the complemented strain of Δ*hisB*; Δ*trpR*, the *trpR* deletion mutant; and Δ*trpR* (*trpR*), the complemented strain of Δ*trpR*. Results were obtained in three independent experiments. Vertical bars represent standard errors.

after 5 and 10 days. Meanwhile, the complemented strains of *trpR* and *hisB* mutants exhibited a wild-type level in this function. These results suggested that mutations of *trpR* and *hisB* reduced the growth ability of *X. oryzae* pv. *oryzicola* in planta.

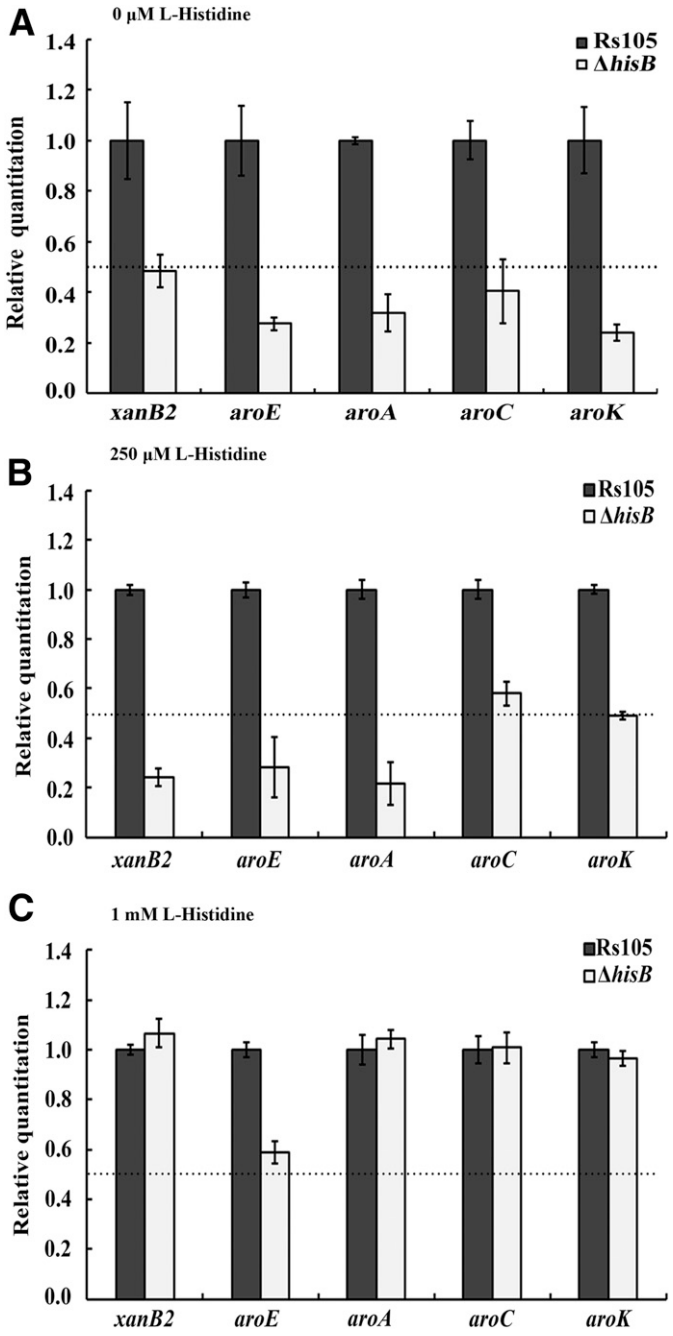

Fig. 8. Transcription determination of five known pigment-associated genes of *Xanthomonas oryzae* pv. *oryzicola* in the *hisB* deletion mutant and wild-type strain. **A,** After treatment with 0 μM L-histidine for 3 h, RNA was isolated from the wild-type strain and mutant of *hisB*. Quantitative real-time PCR was performed to analyze the difference in expression levels of genes (*xanB2*, *aroE*, *aroA*, *aroC*, and *aroK*) between the wild-type and Δ*hisB* mutant. **B,** After treatment with 250 μM L-histidine for 3 h, RNA was isolated from the wild-type strain and mutant of *hisB*. Quantitative real-time PCR was performed to analyze the difference in expression levels of genes (*xanB2*, *aroE*, *aroA*, *aroC*, and *aroK*) between the wild-type and Δ*hisB* mutant. **C,** After treatment with 1 mM L-histidine for 3 h, RNA was isolated from the wild-type strain and the mutant of *hisB*. Quantitative real-time PCR was performed to analyze the difference in expression levels of genes (*xanB2*, *aroE*, *aroA*, *aroC*, and *aroK*) between the wild-type and Δ*hisB* mutant. Data were the means ± standard deviations of triplicate measurements from a representative experiment, and similar data were reported from two other independent experiments. Vertical bars represent standard error. Black dashed line indicates a twofold decrease in the transcription level.

To determine whether the virulence reduction was because of the reduced ability to trigger plant immunity, we tested the ability to trigger HR in the *his* operon mutants. All mutants produced similar level of HR compared with the wild-type, indicating that *his* operon was not involved in the triggering of HR in nonhost (plant) tobacco.

Growth rate of *trpR* and *hisB* mutants in XOM3 supplemented with different concentrations of L-histidine. To confirm the effects of *trpR* and *hisB* on histidine biosynthesis in *X. oryzae* pv. *oryzicola*, we measured the growth rate of wild-type strain Rs105, the *trpR* mutant (Δ*trpR*), the *hisB* mutant (Δ*hisB*), and their corresponding complemented strains in XOM3 supplemented with different concentrations of L-histidine. As shown in Figure 5A, Δ*trpR* and Δ*hisB* displayed reduced growth in XOM3 supplemented with 0 μM L-histidine compared with wild-type strain and corresponding complemented strain. The growth ability of *hisB* mutant in XOM3 was partially restored by supplementing 50 μM and 250 μM L-histidine into the growth medium, whereas the growth ability of the *trpR* mutant remained almost unchanged (Fig. 5B and C). When the concentration of histidine in XOM3 reached 1 mM, the growth rate of Δ*hisB* could be completely restored to the level of the wild-type strain. Using the same conditions, the growth ability of Δ*trpR* was partially restored at 96 h (Fig. 5D). These results supported the assertion that *trpR* and *hisB* were necessary for histidine biosynthesis in *X. oryzae* pv. *oryzicola*.

***trpR* negatively regulates the expression of *hisG*, *-D*, -C, *-B*, *-H*, *-A*, and *-F*, and the transcription of *hisG*, *-D*, -C, *-B*, *-H*, *-A*, *-F*, and *trpR* is inhibited by histidine.** Bioinformatics analysis shows that the *trpR* is located upstream of *hisG* and encodes a transcriptional regulator. In order to investigate the effect of *trpR* on the transcriptional level of other genes of the *his* operon, a quantitative real-time PCR was performed comparing between the wild-type and Δ*trpR* mutant with/without L-histidine. Results showed that the transcription of *hisG*, *-D*, *-C*, *-B*, *-H*, *-A*, and *-F* in Δ*trpR* was higher than in the wild-type strain with 0 μM L-histidine, whereas the expression level of *hisIE* in Δ*trpR* was not significantly different when compared with gene expression of the wild-type strain in same conditions (Fig. 6). After treatment with 250 μM and 1 mM L-histidine for 3 h, we could also observe that the transcription of *hisG*, *-D*, *-C*, *-B*, *-H*, *-A*, and *-F* in Δ*trpR* was higher in comparison with genes expression of the wild-type strain in the same conditions (Fig. 6). Meanwhile, results showed that the transcription of *hisG*, *-D*, -C, *-B*, *-H*, *-A*, and *-F* and *trpR* in wild-type strains treated with 250 μM and 1 mM L-histidine was lower than in the wild-type strain treated with 0 μM L-histidine, whereas the expression level of gene *hisIE* was not significantly different among wild-type strains treated by different concentrations of histidine (Fig. 6). These results indicated that *trpR* negatively regulates the expression of *hisG*, *-D*, *-C*, *-B*, *-H*, *-A*, and *-F*, and the transcription of *hisG*, *-D*, *-C*, *-B*, *-H*, *-A*, and *-F* and *trpR* is inhibited by histidine.

Mutation of *hisB* in *X. oryzae* pv. *oryzicola* impairs xanthomonadins production. The results in Figure 2 showed that the *hisB* mutant phenotypically appeared as a clear white colony as opposed to the yellow colony morphology developed by the wild type. As the yellow pigment produced by *X. oryzae* pv. *oryzicola* is the result of xanthomonadins production, we hypothesized that that *hisB* might be related to xanthomonadins production in *X. oryzae* pv. *oryzicola*. To test this hypothesis, xanthomonadins were extracted from the wild-type, the *hisB* mutant and the complementation strain Δ*hisB* (*hisB*) in XOM3 supplemented with different concentrations of L-histidine. Considering that Δ*hisB* growth at 50 μM concentration of L-histidine was too slow to collect bacteria, we quantified the xanthomonadins production at 250 μM and 1 mM L-histidine. This experiment was also carried out with the *trpR* mutant and its corresponding complemented strain Δ*trpR* (*trpR*). As shown in Figure 7A and C, the extracted xanthomonadins from Δ*hisB* were lighter in color, and

quantitative analysis showed that the xanthomonadins production level of Δ*hisB* was significantly decreased compared with the wild-type strain; however, the xanthomonadins production level of Δ*hisB* could be restored to wild-type level in XOM3 supplemented with 1 mM L-histidine (Fig. 7B and C). Xanthomonadins production level of Δ*trpR* did not significantly decrease compared with the wild-type strain. These results indicated that *hisB* played a role in xanthomonadins production in *X. oryzae* pv. *oryzicola*.

Transcriptional expression of five known pigment-associated genes is reduced in the *hisB* deletion mutant. To investigate the mechanism of *hisB* in affecting xanthomonadins production, transcriptional expression of five pigment-associated genes, including *xanB2* (encodes bifunctional chorismatase), *aroE* (encodes shikimate 5-dehydrogenase), *aroA* (encodes 3-phosphoshikimate1-carboxyvinyltransferase), *aroC* (encodes chorismate synthase), and *aroK* (encodes shikimate kinase) (Guo et al. 2012; Kim et al. 2015; Song et al. 2012; Wang et al. 2007; Zhou et al. 2013a, b) was compared in Δ*hisB* and wild type strains cultured in XOM3 supplemented with different concentrations of L-histidine. This was done to investigate whether *hisB* had a regulatory role for transcriptional expression of these known pigment-associated genes in *X. oryzae* pv. *oryzicola*. The mutation of *hisB* reduced the transcriptional expression of five known pigment-associated genes (*xanB2*, *aroE*, *aroA*, *aroC*, and *aroK*) in XOM3 supplemented with 0 and 250 μM L-histidine (Fig. 8A and B). All selected genes were restored to wild-type expression levels in XOM3 supplemented with 1 mM L-histidine (Fig. 8C).

***aroE* is required for xanthomonadins production and virulence of *X. oryzae* pv. *oryzicola* and the *aroE* is not necessary for triggering the HR in nonhost (plant) tobacco.** To test whether the pigment-associated gene in *X. oryzae* pv. *oryzicola* involved in xanthomonadins production and virulence, we constructed the deletion mutant of *aroE*. As shown in Figure 9A, the mutant of *aroE* showed white color in the plate surface, while the wild-type Rs105 and its corresponding complemented strain showed yellow color. Meanwhile, the mutant of *aroE* exhibited a significant reduction in virulence compared with wild type strain in this function, whereas its corresponding complemented strain retained wild-type ability in this function (Fig. 9B and C). This result indicated that *aroE* was required for xanthomonadins production and virulence *X. oryzae* pv. *oryzicola*. As shown in Supplementary Figure S2, the mutant of *aroE* produced similar level of HR compared with the wild-type, indicating that the *aroE* was not involved in the triggering of HR in nonhost (plant) tobacco.

DISCUSSION

In this study, nine mutants of histidine biosynthesis genes were constructed. Auxotrophic assays confirmed that the *his* operon was involved in histidine biosynthesis in *X. oryzae* pv. *oryzicola*.

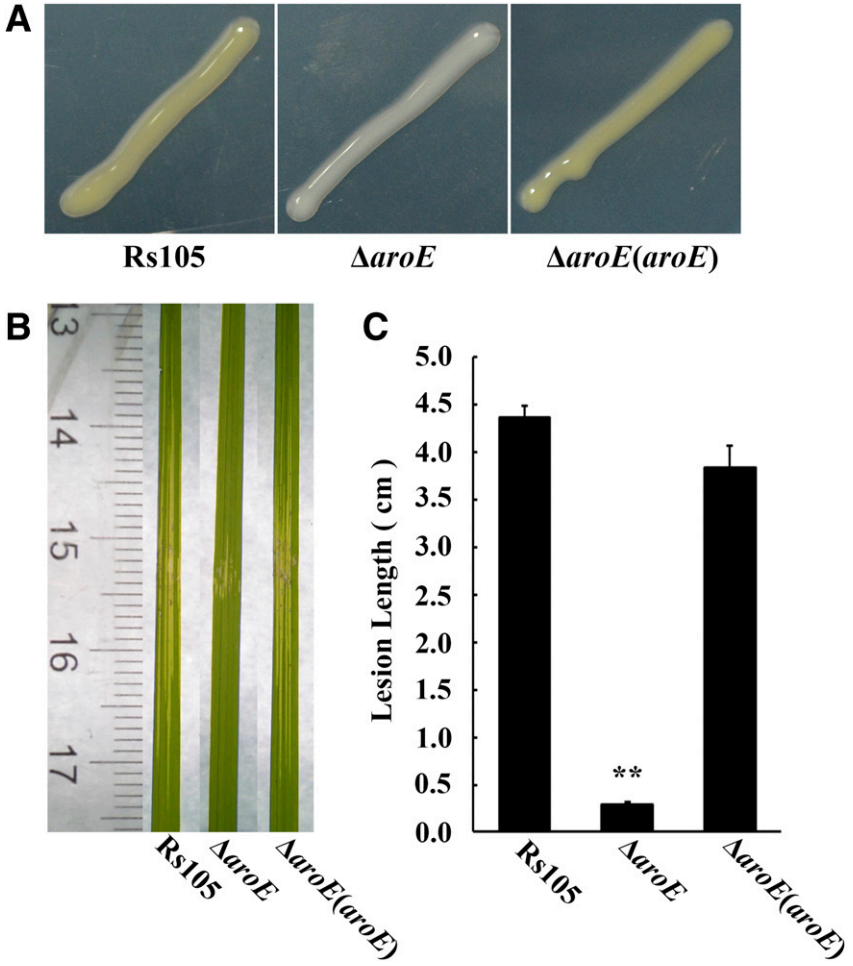

Fig. 9. *aroE* is required for xanthomonadins production and virulence of *Xanthomonas oryzae* pv. *oryzicola*. **A,** Morphological characteristics of *X. oryzae* pv. *oryzicola* strains are shown. **B,** Lesion lengths on the leaves of rice seedlings (cultivar Shanyou63, 2 weeks old) by infiltration with *X. oryzae* pv. *oryzicola* strains. **C,** Calculated data of lesion length on the leaves of rice seedlings (Shanyou63, 2 weeks old) inoculated with *X. oryzae* pv. *oryzicola* strains. Rs105, the wild-type strain of *X. oryzae* pv. *oryzicola*; Δ*aroE*, the *aroE* deletion mutant; and Δ*aroE* (*aroE*), the complemented strain of Δ*aroE*. The experiment was repeated three times. Data were the means ± standard deviations from three repeats, each with 10 leaves. Vertical bars represent standard errors. ** indicates a significant difference between mutant and the wild-type Rs105 at $P = 0.01$.

Mutations of *trpR* and *hisB* impaired the virulence and growth of *X. oryzae* pv. *oryzicola* in planta. Meanwhile, the *hisB* gene was required for xanthomonadins production in *X. oryzae* pv. *oryzicola*. It also demonstrated that the *trpR* gene could negatively regulate the expression of *hisG*, *-D*, *-C*, *-B*, *-H*, *-A*, and *-F*, while transcriptions of *hisG*, *-D*, *-C*, *-B*, *-H*, *-A*, *-F*, and *trpR* could be inhibited by histidine.

The *his* operon was highly conserved both in its genomic organization and gene function among different *Xanthomonas* (Fig. 1). Previous study have shown that HisB and HisIE were both histidine biosynthesis bifunctional proteins, but they had different functions and participated in different reactions in histidine biosynthesis (Alifano et al. 1996). The bifunctional HisIE enzyme, which catalyzes the second and third steps of the histidine biosynthesis pathway, is encoded by *hisIE* and is involved in the activities of two enzymes, namely, phosphoribosyl-ATP pyrophosphatase and phosphoribosyl-AMP cyclohydrolase (Kulis-Horn et al. 2014). *hisB* encodes HisB enzyme, which is a bifunctional enzyme implicated in the imidazoleglycerol-phosphate dehydratase activity, for the sixth step of biosynthesis, and the histidinol-phosphate phosphatase activity, for the eighth step of biosynthesis (Kulis-Horn et al. 2014). Results obtained during this study have shown that *hisB* gene was required for virulence and xanthomonadins production in *X. oryzae* pv. *oryzicola*, but *hisIE* was not required for these functions. Moreover, results showed that the expression of *hisB* was negatively regulated by *trpR* and inhibited by histidine, but the expression of *hisIE* was not significantly affected by *trpR* and histidine (Fig. 6). Further investigation is needed to understand the role of *hisIE* in *X. oryzae* pv. *oryzicola*.

All nine mutants of the *his* operon in *X. oryzae* pv. *oryzicola* could not grow well in XOM3 without histidine and their growth could be partially or completely restored by exogenous addition of histidine (Fig. 2). This result confirmed that the conserved *his* operon was involved in histidine biosynthesis. Interestingly, although nine genes in the *his* operon were necessary for histidine biosynthesis, only the genes of *trpR* and *hisB* were strictly required for the virulence of *X. oryzae* pv. *oryzicola* (Fig. 3). Meanwhile, mutations of *trpR* and *hisB* reduced the in planta growth ability of *X. oryzae* pv. *oryzicola* (Fig. 4). However, we found that the *his* operon did not impair HR, indicating that the contribution of the histidine synthesis pathway to virulence might be not related to HR in *X. oryzae* pv. *oryzicola*. These results indicated that the decrease of *hisB* or *trpR* in symptoms development was associated with the reduced in *planta* growth, and this was supported by the fact that the *his* operon did not impair HR response. Finally, we compared the protease activity of wild-type Rs105 and mutants, but no visible alterations in the hydrolytic zones were detected around the bacterial colonies of the mutants and the wild- type strain. Determination of extracellular protease activity indicated that the *his* operon was independent of protease activity (data not shown).

Bioinformatics analysis showed that *trpR* gene which is located upstream of *hisG* encodes a transcriptional regulator (Fig. 1). In this study, the mutant of *trpR* could not grow well in XOM3 medium with 0 μM L-histidine compared with the wild type, and the growth of *trpR* could not be completely restored by exogenous addition of histidine (Fig. 2). Meanwhile, our data revealed that *trpR* could negatively regulate the expression of *hisA*, *-B*, *-C*, *-D*, *-F*, *-G*, and *-H* (Fig. 6). Thus, we speculated that the overexpression of *his* operon in *trpR* mutant was toxic for the cell, and possible toxic effect could explain why the virulence and bacterial growth in planta of the *trpR* mutant decreased. The transcription of *hisG*, *-D*, -C, *-B*, *-H*, *-A*, and *-F* was inhibited by histidine (Fig. 6). This indicated that histidine could feedback histidine biosynthetic pathways: when external sources of histidine are available, the histidine biosynthesis genes will not be turned on. Moreover, the transcription of *trpR* which acted as a transcriptional repressor to negatively regulate the expression of other genes in the *his* operon could also be inhibited by histidine. The roles of *trpR* of *X. oryzae* pv. *oryzicola* need to be further investigated.

Most *Xanthomonas* bacteria produce membrane-bound yellow pigments known as xanthomonadins (Starr 1981). Xanthomonadins are not only a useful chemotaxonomic and diagnostic marker for *Xanthomonas* spp., but it can also protect the pathogen from photobiological and peroxidation damages in epiphytic survival and in bacterial systemic infections (He et al. 2011; Jenkins and Starr 1982; Poplawsky et al. 2000; Rajagopal et al. 1997; Schaad and Stall 1988; Starr and Stephens 1964).

In this study, we found that deletion of *hisB* significantly reduced the xanthomonadins production compared with the wild-type strain (Fig. 7A and C). Xanthomonadins are closely related to the pathogenicity of *Xanthomonas*. In vitro inoculation experiments showed that the pathogenicity of pigment-deficient mutants of *X. oryzae* pv. *oryzae* or *X. campestris* pv. *campestris* is decreased (Goel et al. 2001; Poplawsky and Chun 1998). In the present study, the mutant of *hisB* not only reduced the xanthomonadins production but also impaired the bacterial virulence of *X. oryzae* pv. *oryzicola*. This finding indicated that xanthomonadins were also closely related to the pathogenicity of *X. oryzae* pv. *oryzicola.* Xanthomonadin biosynthesis is based on the shikimate pathway (He et al. 2011; Jenkins and Starr 1982; Poplawsky et al. 2000; Rajagopal et al. 1997). Our results implied that *hisB* might be related to the shikimate pathway. To test this hypothesis, we identified the transcriptional expression levels of five key shikimate pathway-related genes, such as *aroA* (*XOC_2876*, encodes 3-phosphoshikimate1-carboxyvinyltransferase), *aroC* (*XOC_2961*, encodes chorismate synthase), *aroE* (*XOC_4333*, encodes shikimate 5-dehydrogenase), *aroK* (*XOC_1390*, encodes shikimate kinase), and *XanB2* (*XOC_0424*, encodes shikimate 5-dehydrogenase) (Kim et al. 2015; Song et al. 2012; Zhou et al. 2013b), in Δ*hisB* and wild type. As shown in Figure 8, the deletion of *hisB* reduced the transcriptional expression level of shikimate pathway-related genes (*xanB2*, *aroE*, *aroA*, *aroC*, and *aroK*). This result indicated that *hisB* might be acting through the shikimate pathway to influence the xanthomonadins production. Meanwhile, using the *aroE* mutant, we demonstrated that one of shikimate pathway-related genes, *aroE*, played an important role in xanthomonadin production and virulence in *X. oryzae* pv. *oryzicola*, proving that xanthomonadin was involved in the virulence of *X. oryzae* pv. *oryzicola* (Fig. 9). In addition, our study indicated that *hisB* might be linked to the shikimate pathway and the effect of *hisB* in the virulence was connected with xanthomonadins decrease in *X. oryzae* pv. *oryzicola*.

In summary, this study confirmed that the *his* operon is involved in histidine biosynthesis in *X. oryzae* pv. *oryzicola*. This study also demonstrated that genes *trpR* and *hisB* were required for virulence and bacterial growth in planta, and revealed that these two virulence-associated genes play roles in the regulation of histidine biosynthesis and in the xanthomonadins production, respectively. These findings extend our understanding of histidine metabolic pathways in *Xanthomonas* spp. and in bacterial species in general.

LITERATURE CITED

Alifano, P., Fani, R., Lio, P., Lazcano, A., Bazzicalupo, M., Carlomagno, M. S., and Bruni, C. B. 1996. Histidine biosynthetic pathway and genes: Structure, regulation, and evolution. Microbiol. Rev. 60:44-69.

Bochner, B. R., and Ames, B. N. 1982. ZTP (5-amino 4-imidazole carboxamide riboside 5′-triphosphate): A proposed alarmone for 10-formyl-tetrahydrofolate deficiency. Cell 29:929-937.

Carlomagno, M. S., Chiariotti, L., Alifano, P., Nappo, A. G., and Bruni, C. B. 1988. Structure and function of the *Salmonella typhimurium* and *Escherichia coli* K-12 histidine operons. J. Mol. Biol. 203:585-606.

Chapman, L. F., and Nester, E. W. 1969. Gene–enzyme relationships in histidine biosynthesis in *Bacillus subtilis*. J. Bacteriol. 97:1444-8.

Chiariotti, L., Alifano, P., Carlomagno, M. S., and Bruni, C. B. 1986. Nucleotide sequence of the *Escherichia coli hisD* gene and of the *Escherichia coli* and *Salmonella typhimurium hisIE* region. Mol. Gen. Genet. 203:382-388.

De Feyter, R., Kado, C. I., and Gabriel, D. W. 1990. Small, stable shuttle vectors for use in *Xanthomonas*. Gene 88:65-72.

Fani, R., Lio, P., and Lazcano, A. 1995. Molecular evolution of the histidine biosynthetic pathway. J. Mol. Evol. 41:760-774.

Fani, R., Tamburini, E., Mori, E., Lazcano, A., Lio, P., Barberio, C., Casalone, E., Cavalieri, D., Perito, B., and Polsinelli, M. 1997. Paralogous histidine biosynthetic genes: Evolutionary analysis of the *Saccharomyces cerevisiae* HIS6 and HIS7 genes. Gene 197:9-17.

Fink, G. R. 1964. Gene-enzyme relations in histidine biosynthesis in yeast. Science 146:525-527.

Goel, A. K., Rajagopal, L., and Sonti, R. V. 2001. Pigment and virulence deficiencies associated with mutations in the *aroE* gene of *Xanthomonas oryzae* pv. *oryzae*. Appl. Environ. Microbiol. 67:245-250.

Guo, W., Cui, Y. P., Li, Y. R., Che, Y. Z., Yuan, L., Zou, L. F., Zou, H. S., and Chen, G. Y. 2012. Identification of seven *Xanthomonas oryzae* pv. *oryzicola* genes potentially involved in pathogenesis in rice. Microbiology-Sgm. 158: 505-518.

He, Y. W., Wu, J., Zhou, L., Yang, F., He, Y. Q., Jiang, B. L., Bai, L., Xu, Y., Deng, Z., Tang, J. L., and Zhang, L. H. 2011. *Xanthomonas campestris* diffusible factor is 3-hydroxybenzoic acid and is associated with xanthomonadin biosynthesis, cell viability, antioxidant activity, and systemic invasion. Mol. Plant-Microbe Interact. 24:948-957.

Jenkins, C. L., and Starr, M. P. 1982. The pigment of *Xanthomonas populi* is a nonbrominated aryl-heptaene belonging to xanthomonadin pigment group II. Curr. Microbiol. 7:195-198.

Jung, S., Chun, J. Y., Yim, S. H., Lee, S. S., Cheon, C. I., Song, E., and Lee, M. S. 2010. Transcriptional regulation of histidine biosynthesis genes in *Corynebacterium glutamicum*. Can. J. Microbiol. 56:178-187.

Jung, S. I., Han, M. S., Kwon, J. H., Cheon, C. I., Min, K. H., and Lee, M. S. 1998. Cloning of the histidine biosynthetic genes of *Corynebacterium glutamicum*: Organization and sequencing analysis of the *hisA*, *impA*, and *hisF* gene cluster. Biochem. Biophys. Res. Commun. 247:741-745.

Kim, H. I., Noh, T. H., Lee, C. S., and Park, Y. J. 2015. A mutation in the *aroE* gene affects pigment production, virulence, and chemotaxis in *Xanthomonas oryzae* pv. *oryzae*. Microbiol. Res. 170:124-130.

Klem, T. J., and Davisson, V. J. 1993. Imidazole glycerol phosphate synthase: The glutamine amidotransferase in histidine biosynthesis. Biochemistry 32: 5177-5186.

Kulis-Horn, R. K., Persicke, M., and Kalinowski, J. 2014. Histidine biosynthesis, its regulation and biotechnological application in *Corynebacterium glutamicum*. Microbiol. Biotechnol. 7:5-25.

Lee, H. S., Cho, Y., Lee, J. H., and Kang, S. G. 2008. Novel monofunctional histidinol-phosphate phosphatase of the DDDD superfamily of phosphohydrolases. J. Bacteriol. 190:2629-2632.

Liang, X., Yu, X., Pan, X., Wu, J., Duan, Y., Wang, J., and Zhou, M. 2018. A thiadiazole reduces the virulence of *Xanthomonas oryzae* pv. *oryzae* by inhibiting the histidine utilization pathway and quorum sensing. Mol. Plant Pathol. 19:116-128.

Niño-Liu, D. O., Ronald, P. C., and Bogdanove, A. J. 2006. *Xanthomonas oryzae* pathovars: Model pathogens of a model crop. Mol. Plant Pathol. 7:303-324.

Papaleo, M. C., Russo, E., Fondi, M., Emiliani, G., Frandi, A., Brilli, M., Pastorelli, R., and Fani, R. 2009. Structural, evolutionary and genetic analysis of the histidine biosynthetic "core" in the genus *Burkholderia*. Gene 448:16-28.

Park, Y. J., Song, E. S., Kim, Y. T., Noh, T. H., Kang, H. W., and Lee, B. M. 2007. Analysis of virulence and growth of a purine auxotrophic mutant of *Xanthomonas oryzae* pathovar *oryzae*. FEMS Microbiol. Lett. 276:55-59.

Polgár, L. 2005. The catalytic triad of serine peptidases. Cell. Mol. Life Sci. 62:2161-2172.

Poplawsky, A. R., and Chun, W. 1998. *Xanthomonas campestris* pv. *campestris* requires a functional pigB for epiphytic survival and host infection. Mol. Plant-Microbe Interact. 11:466-475.

Poplawsky, A. R., Urban, S. C., and Chun, W. 2000. Biological role of xanthomonadin pigments in *Xanthomonas campestris* pv. *campestris*. Appl. Environ. Microbiol. 66:5123-5127.

Qian, G., Liu, C., Wu, G., Yin, F., Zhao, Y., Zhou, Y., Zhang, Y., Song, Z., Fan, J., Hu, B., and Liu, F. 2013a. AsnB, regulated by diffusible signal factor and global regulator Clp, is involved in aspartate metabolism, resistance to oxidative stress and virulence in *Xanthomonas oryzae* pv. *oryzicola*. Mol. Plant Pathol. 14:145-157.

Qian, G., Zhou, Y., Zhao, Y., Song, Z., Wang, S., Fan, J., Hu, B., Venturi, V., and Liu, F. 2013b. Proteomic analysis reveals novel extracellular virulence-associated proteins and functions regulated by the diffusible signal factor (DSF) in *Xanthomonas oryzae* pv. *oryzicola*. J. Proteome Res. 12: 3327-3341.

Rajagopal, L., Sundari, C. S., Balasubramanian, D., and Sonti, R. V. 1997. The bacterial pigment xanthomonadin offers protection against photodamage. FEBS Lett. 415:125-128.

Rebek, J. 1990. On the structure of histidine and its role in enzyme active sites. Struct. Chem. 1:129-131.

Schaad, N. W., and Stall, R. E. 1988. *Xanthomonas*. Pages 81-94 in: Laboratory Guide for Identification of Plant Pathogenic Bacteria, 2nd ed. N. W. Schaad, ed. American Phytopathological Society, St. Paul, MN.

Song, E. S., Park, Y. J., Noh, T. H., Kim, Y. T., Kim, J. G., Cho, H., and Lee, B. M. 2012. Functional analysis of the *aroC* gene encoding chorismate synthase from *Xanthomonas oryzae* pathovar *oryzae*. Microbiol. Res. 167: 326-331.

Starr, M. P. 1981. The genus *Xanthomonas*. Pages 742-763 in: The Prokaryotes. M. P. Starr, H. Stolp, H. G. Trüper, A. Balows, and H. G. Schlegel, eds. Vol. 1. Springer Verlag, Berlin.

Starr, M. P., and Stephens, W. L. 1964. Pigmentation and taxonomy of the genus *Xanthomonas*. J. Bacteriol. 87:293-302.

Stepansky, A., and Leustek, T. 2006. Histidine biosynthesis in plants. Amino Acids 30:127-142.

Wang, L., Makino, S., Subedee, A., and Bogdanove, A. J. 2007. Novel candidate virulence factors in rice pathogen *Xanthomonas oryzae* pv. *oryzicola* as revealed by mutational analysis. Appl. Environ. Microbiol. 73: 8023-8027.

Wiater, A., Krajewska-Grynkiewicz, K., and Klopotowski, T. 1971. Histidine biosynthesis and its regulation in higher plants. Acta Biochim. Pol. 18: 299-307.

Zhao, Y., Qian, G., Fan, J., Yin, F., Zhou, Y., Liu, C., Shen, Q., Hu, B., and Liu, F. 2012. Identification and characterization of a novel gene, *hshB*, in *Xanthomonas oryzae* pv. *oryzicola* co-regulated by quorum sensing and clp. Phytopathology 102:252-259.

Zhao, Y., Qian, G., Yin, F., Fan, J., Zhai, Z., Liu, C., Hu, B., and Liu, F. 2011. Proteomic analysis of the regulatory function of DSF-dependent quorum sensing in *Xanthomonas oryzae* pv. *oryzicola*. Microbiol. Pathog. 50:48-55.

Zhou, L., Huang, T. W., Wang, J. Y., Sun, S., Chen, G., Poplawsky, A., and He, Y. W. 2013a. The rice bacterial pathogen *Xanthomonas oryzae* pv. *oryzae* produces 3-hydroxybenzoic acid and 4-hydroxybenzoic acid by XanB2 for use in xanthomonadin, ubiquinone, and exopolysaccharide biosynthesis. Mol. Plant-Microbe Interact. 26:1239-1248.

Zhou, L., Wang, J. Y., Wu, J., Wang, J., Poplawsky, A., Lin, S., Zhu, B., Chang, C., Zhou, T., Zhang, L. H., and He, Y. W. 2013b. The diffusible factor synthase XanB2 is a bifunctional chorismatase that links the shikimate pathway to ubiquinone and xanthomonadins biosynthetic pathways. Mol. Microbiol. 87:80-93.

Zou, L. F., Li, Y. R., and Chen, G. Y. 2011. A non-marker mutagenesis strategy to generate poly-*hrp* gene mutants in the rice pathogen *Xanthomonas oryzae* pv. *oryzicola*. Agric. Sci. China 10:1139-1150.

Zou, L. F., Wang, X. P., Xiang, Y., Zhang, B., Li, Y. R., Xiao, Y. L., Wang, J. S., Walmsley, A. R., and Chen, G. Y. 2006. Elucidation of the *hrp* clusters of *Xanthomonas oryzae* pv. *oryzicola* that control the hypersensitive response in nonhost tobacco and pathogenicity in susceptible host rice. Appl. Environ. Microbiol. 72:6212-6224.